



HAL
open science

ELASTIC CONSTANTS AND INTERNAL FRICTION OF REINFORCED COMPOSITES

H. Ledbetter

► **To cite this version:**

H. Ledbetter. ELASTIC CONSTANTS AND INTERNAL FRICTION OF REINFORCED COMPOSITES. Journal de Physique Colloques, 1985, 46 (C10), pp.C10-573-C10-578. 10.1051/jphyscol:198510128 . jpa-00225331

HAL Id: jpa-00225331

<https://hal.science/jpa-00225331>

Submitted on 4 Feb 2008

HAL is a multi-disciplinary open access archive for the deposit and dissemination of scientific research documents, whether they are published or not. The documents may come from teaching and research institutions in France or abroad, or from public or private research centers.

L'archive ouverte pluridisciplinaire **HAL**, est destinée au dépôt et à la diffusion de documents scientifiques de niveau recherche, publiés ou non, émanant des établissements d'enseignement et de recherche français ou étrangers, des laboratoires publics ou privés.

ELASTIC CONSTANTS AND INTERNAL FRICTION OF REINFORCED COMPOSITES

H.M. LEDBETTER

Fracture and Deformation Division, Center for Materials Science, National Bureau of Standards, Boulder, Colorado 80303, U.S.A.

Abstract - We describe experimental studies on the anisotropic elastic constants and internal friction of reinforced composites. Reinforcement types include fiber and fabric. Studied materials include boron-aluminum, glass-epoxy, boron-epoxy, graphite-epoxy, and aramid-epoxy. We made most measurements with a Marx three-component oscillator at kilohertz frequencies. In all cases, elastic-constant direction dependence fit relationships derived for homogeneous monocrystals. Usually, elastic stiffness and internal friction show an inverse relationship. In no case did the inclusion-matrix interface appear to contribute significantly to internal friction.

I - INTRODUCTION

A physical property of a composite material depends mainly on three ingredients: matrix property, inclusion property, and phase geometry. Phase geometry includes many variables: volume fraction, inclusion shape, inclusion orientation, inclusion size, and inclusion distribution. For some composites, especially at higher temperatures, the inclusion-matrix interface affects a physical property.

The present study considers two strongly related physical properties: elastic constants and internal friction. Especially, we focus on Young modulus, E , and internal friction, Q^{-1} , determined in rod-shaped specimens in a Young-modulus (extensional-wave) mode.

Elastic constants enter many aspects of composite-material behavior: stiffness-weight ratio, load-deflection, elastic instability, thermoelastic stress, residual stress, sound-wave velocities, material characterization, relationship to other physical properties (for example, thermal expansivity and specific heat), plastic deformation, theoretical strength, and nondestructive evaluation.

Internal friction of composites relates to many of the above phenomena. In addition, it relates especially to structural damping and to detection of premonitory failure as manifested in cracking and delamination.

II - EXPERIMENT

We measured Young modulus and Young-modulus-mode internal friction using a Marx three-component oscillator in the kilohertz-frequency region /1/. In this method, the Young-modulus value arises from the specimen resonance frequency and the internal friction from the half-power width of the resonance peak. Typical specimens were cylindrical rods 5 mm in diameter and 2 to 10 cm long.

III - RESULTS

Table 1 gives ambient-temperature results for several fiber-reinforced and cloth-reinforced composites. Figure 1 shows a log-log plot of most of these results. Figure 2 shows the angular variation of E and Q^{-1} for a uniaxial boron-fiber-reinforced aluminum-matrix composite. For the warp-fill plane, Fig. 3 shows a similar diagram for a glass-fiber-cloth-reinforced epoxy-matrix composite. Figure 4 shows a similar diagram for the Young modulus of a graphite-fiber-cloth-reinforced epoxy-matrix composite.

IV - DISCUSSION

Figure 1 shows an approximately hyperbolic relationship between Young modulus and internal friction. If we assume a relationship

$$E^n Q^{-1} = C = \text{constant} \quad (1)$$

then with E in units of 10^{11} N/m² and Q^{-1} in units of 10^{-4} , a least-squares fit gives $n = 0.80$ and $C = 14.3$. Although this preliminary empirical $E-Q^{-1}$ relationship requires further study, it suggests a useful guideline for understanding and optimizing these two physical properties in fiber-reinforced composites.

For a transverse-isotropic-symmetry material, with the unique axis along x_3 , the Young modulus is

$$E^{-1} = S_{33}' = S_{33} \gamma^4 + S_{11}(1 - \gamma^2)^2 + (2S_{13} + S_{44})\gamma^2(1 - \gamma^2) \quad (2)$$

where S_{ij} denote the Voigt elastic compliances, γ denotes the angle between the unique axis and the specimen axis, and the prime denotes rotation away from the x_3 axis. Composites containing parallel fibers distributed either randomly or triangularly in the transverse plane should exhibit transverse-isotropic symmetry. Figure 2 shows that measurements on a boron-aluminum composite fit the predictions of Eq. (2). Also, Fig. 2 shows an inverse relationship between the directional variations of E and Q^{-1} : the minimum in E corresponds to the maximum in Q^{-1} , and vice versa. This extends the general result shown in Fig. 1 for principal directions. Presently, we do not understand the irregular $Q^{-1}(\gamma)$ behavior. We speculate that this may arise from mode coupling related to the composite's laminated structure.

For an orthotropic-symmetry material, with principal axes along x_1, x_2, x_3 , the Young modulus (in the x_1 - x_2 plane, for example) is

$$E^{-1} = S_{11}' = a_{11}^4 S_{11} + a_{12}^4 S_{22} + a_{11}^2 a_{12}^2 (2S_{12} + S_{66}) \quad (3)$$

where the a_{ij} represent the direction cosines between the specimen axis and the principal axes. Laminated cloth-reinforced composites with 90° angles between warp-direction and fill-direction fibers should exhibit orthotropic macroscopic symmetry. For glass-epoxy, Fig. 3 confirms that the measurements fit Eq. (3). This figure also shows Q^{-1} , which, like the boron-aluminum case, relates inversely to E. Figure 4 shows results for a graphite-cloth-reinforced epoxy-matrix case. The Young

modulus behaves similarly to the glass-epoxy case shown in Fig. 3. Our preliminary measurements show that Q^{-1} for graphite-cloth-epoxy does not vary as expected with angle.

V - CONCLUSIONS

From this study, there arise several conclusions:

1. Composites reinforced with unidirectional fibers exhibit transverse-isotropic symmetry. Composites reinforced with cloth laminae exhibit orthotropic symmetry. One can describe both cases using standard relationships derived for anisotropic monocrystals.
2. Usually, but not always, Q^{-1} decreases when E increases. This inverse relationship tends to hold for three situations: a single composite where inclusion volume fraction changes, among various composites, and within a single composite versus direction.
3. At ambient temperatures, in all composites studied to date (including others not reported here), we found no interface contribution to internal friction.

ACKNOWLEDGMENT

Our composites studies received support from several sponsors, especially DARPA and the DoE Office of Fusion Energy. M. W. Austin made most of the measurements.

REFERENCE

- /1/ Ledbetter, H. M., Cryogenics 20 (1980) 637-640.

TABLE 1. Young modulus and internal friction of several fibrous composites at ambient temperature.

No.	Material	Fiber orientation, degrees	Dynamic Young's modulus, GPa	Internal friction, $Q^{-1} \cdot 10^{-4}$	First-harmonic frequency, kHz	
1	Boron-aluminum	0	226.2 ± 0.2	5.6 ± 0.4	50	
2		90	139.2 ± 0.2	17.0 ± 0.5	80	
3	Boron-epoxy	0	226. ± 4	17.6 ± 1.4	55	
4		90	22.7 ± 0.2	400.8 ± 20.6	35	
5		0, ± 45, 90	121.4 ± 0.8	79.9 ± 3.3	70	
	Glass-epoxy	0	44.3	---	30	
6		Glass-cloth-epoxy 1	woof	30.6 ± 0.6	62.1 ± 8.2	40
7	Glass-cloth-epoxy 2	woof	29.6 ± 0.2	64.9 ± 7.5	40	
		Glass-cloth-epoxy 3	woof	44.3 ± 0.5	5.4 ± 0.3	30
8		Glass-cloth-epoxy 4	warp	29.4 ± 1.0	68.7 ± 6.6	40-70
9	Glass-cloth-epoxy 5	fill	26.3 ± 1.0	100.1 ± 7.8	45-90	
10		normal	14.0 ^a	228.6	55	
11		Glass-cloth-epoxy 6	warp	31.4 ± 0.4	114.5 ± 13.9	40-70
12	Graphite-epoxy 1	fill	27.7	221.6 ± 85.3	40-70	
13		normal	15.6 ± 0.6	406.5	60	
		0	133.5	11.1	90	
	Graphite-epoxy 2	90	10.0	164.2	45	
		± 45			---	
14		Graphite-epoxy 3	0	300.5 ± 0.4	17.9 ± 0.4	65
15	Graphite-epoxy 4	90	7.3 ± 0.5	258.8 ± 0.5	45	
16		0, ± 45, 90	120.0 ± 4.0	44.2 ± 4.0	50	
		0	177. ± 4	15.0 ± 3.8	50	
18	Graphite-epoxy 5	90	8.5	218.0 ± 11.7	30	
19		0, ± 45, 90	70. ± 1	49.8 ± 2.1	40	
20		Graphite-epoxy 6	0	130.4 ± 1	2.8 ± 0.4	60
21	Graphite-epoxy 7	0	130. ± 1	---	60	
		Graphite-cloth epoxy	warp	73.7	274	50
			fill	64.7	320	50
			normal	13.0	1584	50
	Graphite-epoxy 8	0	133.5	11.1	90	
		90	10.0	164.2	45	
22	Aramid-epoxy	0	66.1 ± 0.5	114.8 ± 6.1	60	

^aUncertainties do not occur for some cases because only one specimen was measured.

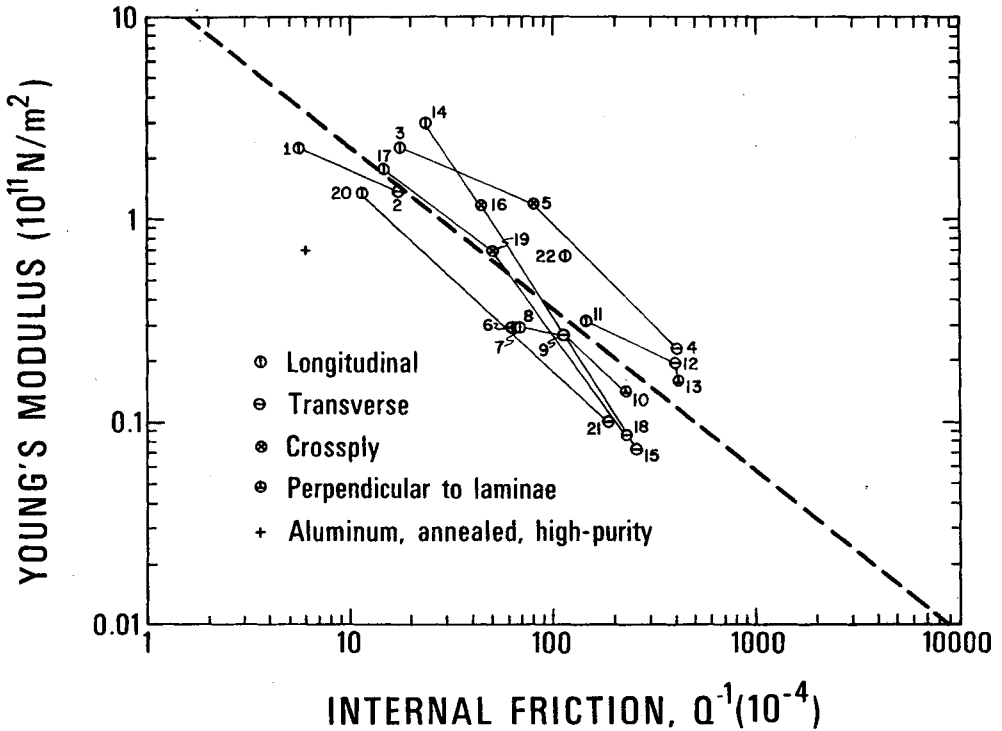


Fig. 1 - Young modulus versus internal friction for fiber-reinforced composite materials in Table 1.

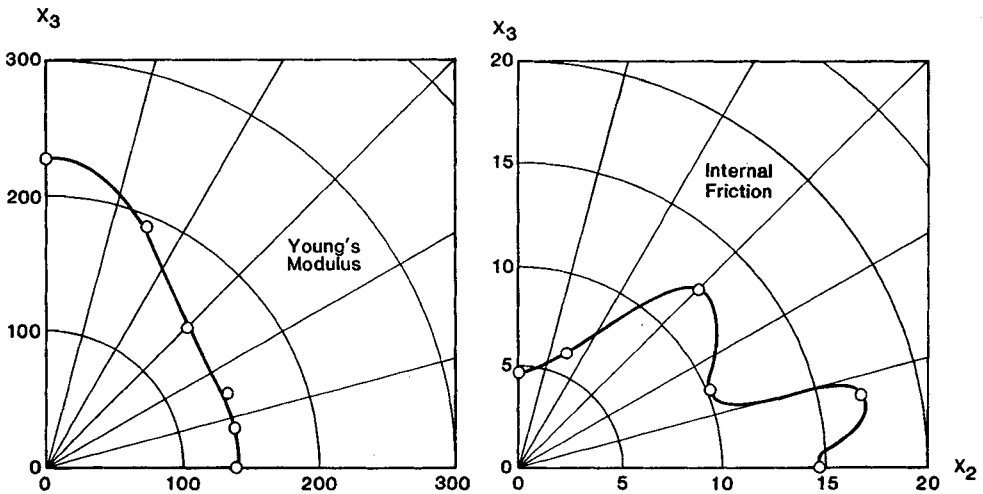


Fig. 2 - Directional variation of Young modulus and internal friction for a uniaxial-boron-fiber aluminum-matrix composite. Fibers lie along x_3 axis. The curve represents Eq. (2).

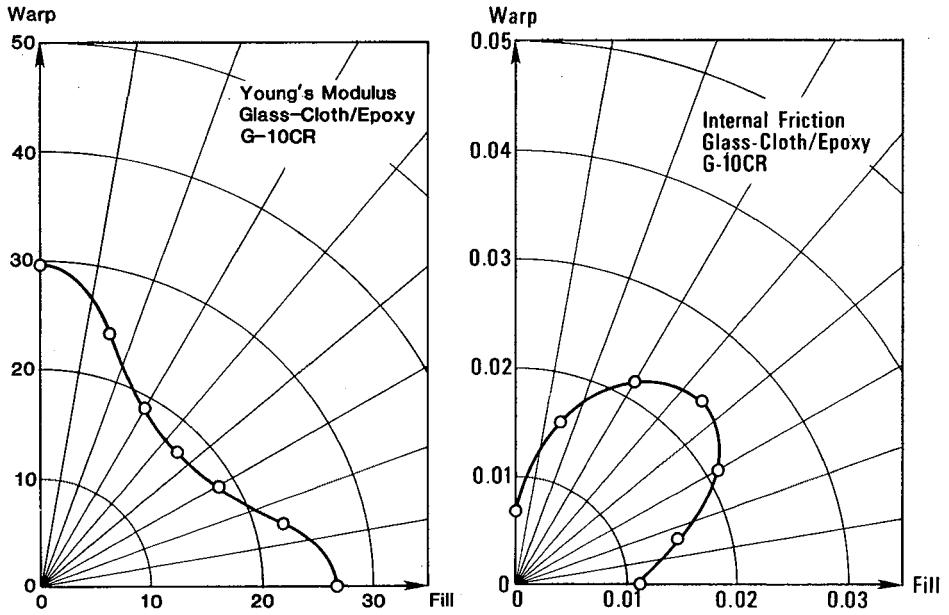


Fig. 3 - Directional variation of Young modulus and internal friction for a glass-fiber-cloth epoxy-matrix laminated composite. Fibers lie in warp and fill directions. The curve represents Eq. (3).

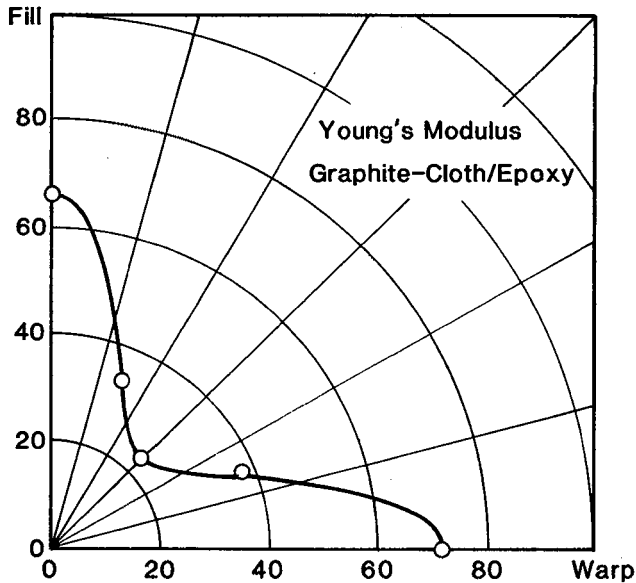


Fig. 4 - Directional variation of Young modulus for a graphite-fiber-cloth epoxy-matrix laminated composite. Fibers lie in warp and fill directions. The curve represents Eq. (3).